

# QUANTITATIVE TEXTURAL PARAMETER SELECTION FOR RESIDENTIAL EXTRACTION FROM HIGH-RESOLUTION REMOTELY SENSED IMAGERY

J. Gu<sup>a,b\*</sup>, J. Chen<sup>a</sup>, Q.M. Zhou<sup>c</sup>, H.W. Zhang<sup>a</sup>, L. Ma<sup>d</sup>

<sup>a</sup>National Geomatics Center of China, Baishengcun, Zizhuyuan, Haidian District, Beijing, China-  
julietgujan@163.com

<sup>b</sup>Beijing Institute of Surveying and Mapping, 15 Yangfangdianlu, Haidian District, Beijing, China

<sup>c</sup>Department of Geography, Hongkong Baptist University, Kowloon Tong, Kowloon, Hong Kong, China

<sup>d</sup>School of Remote Sensing and Information Engineering, Wuhan University, China

**KEY WORDS:** Texture, Residential Area, JM-Distance, Window Size, Quantization Level, Displacement, Orientation

## ABSTRACT:

Residential areas show plenty of texture information on high resolution remotely sensed imagery. Appropriate description about this texture information for discriminating residential class and its background is a key problem for improving the classification results. Method for selecting proper texture parameters is presented in this paper. Based on the analysis of residential texture, grey level co-occurrence matrix (GLCM) and edge density (ED) approaches with candidate nine texture measurements (contrast, homogeneity, dissimilarity entropy, energy, mean, standard deviation, correlation and edge density) is selected as candidate texture measurements. The texture parameters are selected based on separability measured by Jeffries-Matusita distance (JM distance) between residential and its background in corresponding texture space. IKONOS panchromatic imagery has been used as example and the optimal texture parameters were selected by using the proposed method.

## 1. INTRODUCTION

Texture is an important image feature used in visual interpretation of residential area from high-resolution remotely sensed imagery. It is a property that relates to the nature of the variability of pixel values (Anys and He, 1995) which requires elaborate prior models that guide procedures for extraction. Several studies have addressed that the addition of image texture improves image classification. Karathanassi *et al.* (2000) reported that the density of buildings can be discriminated based on a simple, binary co-occurrence matrix. Myint and Lam (2005) used lacunarity as a texture measure to improve traditional spectral based classification accuracy. Gong and Howarth (1990) applied edge detection and smoothing techniques to generate a spatial pseudo-spectral 'road-density' band to supplement conventional spectral bands in classification. Zhang *et al.* (2003) applied a similar approach to study urban change in Beijing. In this case, line rather than edge detection was applied since the former conforms to road patterns better.

Despite the fact that texture can be visually discriminated, there is still no appropriate model for texture. It is more difficult to quantify texture than spectral information as it involves measurements of variability, pattern, shape and size (Coburn and Roberts, 2004). There are two distinct types of methods to extract texture information from an image, i.e. segmentation-based and window-based. The segmentation-based methods firstly segment an image into non-overlapping homogeneous regions (segments), and then texture values are computed from these segments. Such methods assume that residential areas are homogenous and it can be obtained through segmentation algorithms. However, most real residential regions in high-resolution remotely sensed imagery do not present homogeneous features. It is difficult to obtain "pure" residential regions through segmentation algorithms. Another problem of segmentation-based method is that texture values are usually sensitive to the scale, but regions obtained from segmentation

are commonly with different sizes, so that the texture parameters computed from these regions are not comparable. The window-based method is the most prevalent technique. Texture values is calculated from moving a fixed-size, odd-numbered window through the image. The selection of window size is important for computing texture parameters. Besides, since most of texture is computed based on statistics, different texture measurements also have different parameters needs to be pre-set.

In this paper, the evaluation and optimization of parameters for computing textural features to discriminate residential areas from their background class based on Jeffries-Matusita distance (JM-distance) is presented. Section 2 will introduce the texture features and parameter selection method used in this paper. Section 3 will give an example of the selection of texture parameters by using IKONOS Panchromatic imagery. Conclusions will be made in the final section.

## 2. METHODOLOGY

### 2.1 Candidate texture measurements for residential areas

The Haralick grey-level co-occurrence matrix (*GLCM*) is one of the most popular methods for pixel variation statistics (Conners and Harlow 1980). It uses a spatial co-occurrence matrix that computes the relationships of pixel values in a certain window size and uses these values to compute the second-order statistical properties from these matrices (Haralick, 1979). Eight second-order statistics derived from GLCM are mostly used in remote sensing imagery analysis. They are contrast (*CON*), homogeneity (*HOMO*), dissimilarity (*DIS*), entropy (*ENT*), energy (also called angular second moment, *ASM*), mean (*MEAN*), standard deviation (*SD*) and correlation (*COR*). Details about the GLCM method are available in Haralick *et al.* (1979). Equation 1 shows their definitions.

$$\left\{ \begin{array}{l}
 CON = \sum_i \sum_j P(i-j)^2 \\
 HOMO = \sum_i \sum_j \frac{P(i,j)}{1+(i-j)^2} \\
 DIS = \sum_i \sum_j |i-j|P(i,j) \\
 ENT = \sum_i \sum_j P(i,j)[- \log P(i,j)] \\
 ASM = \sum_i \sum_j P^2(i,j) \\
 MEAN = \sum_i \sum_j i \bullet P(i,j) \\
 SD = \sqrt{\sum_i \sum_j P(i-MEAN)^2} \\
 COR = \sum_i \sum_j \frac{(i-MEAN)(j-MEAN)}{SD^2}
 \end{array} \right. \quad (1)$$

Where  $i$  and  $j$  are two different grey levels of the image,  $P$  is the number of the co-appearance of grey levels  $i$  and  $j$ .

Edge density ( $ED$ ) is usually computed through the number of edge pixels in a given window divided by the window size (Equation 2). The detection of edge pixels is the key issue in  $ED$  computing. There are a variety of algorithms have been proposed for edge detection. Among them, Canny edge detection operator (Canny, 1986) is one of effective method. It formulated edge detection as an optimization problem and defines an optimal filter, which can be efficiently approximated by the first derivative of Gaussian function in the one-dimension case. In this study, edge detection by the Canny edge detection operator was performed and a binary edge image (edge pixel is coded as '1', and non-edge pixel is coded as '0') was produced. Then,  $ED$  can be computed based on the binary edge image.

$$ED(x,y) = \frac{1}{W} \sum_{k=-W/2}^{W/2} \sum_{l=-W/2}^{W/2} g(x+k,y+l) \quad (2)$$

Where  $W$  is the window size.  $g(x,y)$  is the pixel value in the given window.

## 2.2 Parameters effect on texture

Although absolute values of texture features had little meaning, it was worthwhile to understand how each feature varied with varying parameters given an image acquisition configuration. This should provide users with the knowledge with which to make a good selection of parameter values instead of testing all possible combinations. The following four parameters need to be pre-set for designing the texture features introduced above.

### 2.2.1 Window size

The moving window size used to calculate texture is a key parameter. In texture analysis, one of the main problems is that

the textural features whose differences will be used to characterize various class types need to be extracted over a local area of unknown size and shape. If this information is gathered over areas that are not large enough with respect to the texture elements or variations, then one cannot expect these local analyses to provide feature values that are invariant across the textured region. Consequently, it is desirable to extract the textural information over as larger an area as possible. If this is the case (i.e. texture features are not calculated from a single texture class), the features would be representing a hybrid values. This problem is similar to mixed-pixel problem and may be termed as mixed-textel problem (Shaban and Dikshit, 2001). Therefore, the need for a large window size results in a trade-off between large window sizes that give stable texture measures and the increasing proportion of between-class variance texture pixels such large windows produce.

### 2.2.2 Quantization level

The dimension of a GLCM is determined by the maximum gray value of the pixel. The more levels included in the computation, the more accurate the extracted textural information, of course, a subsequent increased computation cost (Soh and Tsatsoulis, 1999). Some of the major quantization schemes are uniform quantization, Gaussian quantization and equal probability quantization. The uniform quantization scheme is the simplest, in which gray levels are quantized into separate bins with uniform tolerance limits with no regard to the gray level distribution of the image. This technique is not always preferable. The Gaussian quantization technique is one such scheme. The grey level distribution of the original image is assumed to behave normally. Each quantization bin has the same area under the curve and thus different space smaller spaces in the middle of the distribution and larger spaces at the tails of the distribution. In the equal probability quantization scheme, each bin has similar probability and it has been shown to represent accurate representation of the original image in terms of textural based on GLCM (Connors and Harlow 1978). The Gaussian quantization scheme assume a Gaussian grey level distribution, which is not always true for high-resolution imagery. Equal probability quantization normalizes different image samples so that a bright feature and a dark feature, given the same texture, would have the same co-occurrence matrix, which is undesirable since grey value is important in residential analysis. Thus, in our experiment, we have focused on the uniform quantization scheme.

### 2.2.3 Displacement

The displacement parameter  $\delta$  is important in computation of GLCM. Applying large displacement value to a fine texture would yield a GLCM that does not capture detailed textural information, and vice versa (Soh Tsatsoulis, 1999).

### 2.2.4 Orientation

Every pixel has eight neighboring pixels allowing eight choices for  $\theta$ , which are  $0^\circ, 45^\circ, 90^\circ, 135^\circ, 180^\circ, 225^\circ, 270^\circ$  or  $315^\circ$ . However, taking into consideration the definition of GLCM, the co-occurring pairs obtained by choosing  $\theta$  equal to  $0^\circ$  would be similar to those obtained by choose  $\theta$  equal to  $180^\circ$ . This concept extends to  $45^\circ, 90^\circ$  and  $135^\circ$  as well. Hence, one has four choices to select the value of  $\theta$ . Sometimes, when the image is isotropic, or directional information is not required, one can obtain isotropic GLCM by integration over all angles.

### 2.3 Optimal parameters selection based on JM-distance

The performance of a parameter value of texture features can be evaluated through its effectiveness in classification. The probability of classification error is used to decide the selection of optimal parameters. The smaller the probability of classification error is, the better the parameter value. However, the classification error method need a lot of computation time especially more candidate values for a certain parameter. For the statistical separability of classes is inversely proportional to the probability of error, people turn to use statistical separability of class as texture parameter selection criterion. For example, the divergence criterion, the transformed divergence criterion, the Bhattacharyya distance and the Jeffreys-Matusita (JM) distance are most widely used criteria (Swain and Davis, 1978).

The JM-distance is an appropriate technique of measuring the average separability between different classes. It behaves much more like probability of correct classification (Swain et al.1971). For two densities  $p_1(x)$  and  $p_2(x)$ , the JM-distance  $J$  is given by

$$J = \int_x \left[ \sqrt{p_1(x)} - \sqrt{p_2(x)} \right]^2 dx \quad (3)$$

Which can also be written in the form

$$J = 2(1 - e^{-B_{12}}) \quad (4)$$

In which  $B_{12}$  (Bhattacharyya distance) is given by

$$BD = \frac{1}{8} [\mu_1 - \mu_2]^T \left[ \frac{\Sigma_1 + \Sigma_2}{2} \right]^{-1} [\mu_1 - \mu_2] + \frac{1}{2} \ln \left[ \frac{1}{2} \frac{|\Sigma_1 + \Sigma_2|}{\sqrt{|\Sigma_1| |\Sigma_2|}} \right] \quad (5)$$

Where  $\mu_i$  is the mean vector for class  $i$  and  $\Sigma_i$  is the corresponding class covariance matrix. Since  $0 < e^{-B_{12}} < 1$ ,  $J$  ranges from 0 to 2 with 2 corresponding to the largest separation.

In this paper, to evaluate and optimize of parameters for computing textural features to discriminate residential areas from their background class, the JM-distance is used. The procedure can be achieved through four steps:

- (1) For those textures which have more than one parameter, multiple texture images were produced by changing each parameter of texture features with fixed all other parameters;
- (2) Selecting appropriate samples of residential class and background class from each texture image computed from candidate values, separately. A set of JM-distances will be obtained according to formula (4) and (5);
- (3) Making a statistics of JM-distances changes;
- (4) The optimum parameter value is then determined by those with the largest JM-distance values.

$$J_{optimal} = \max(J_i) \quad (6)$$

Where  $i$  is the number of candidate values.

### 3. RESULTS AND DISCUSSION

An IKONOS panchromatic imagery that has a spatial resolution of 1 meter was used for the experiment. The image covers the test area of Wangjing District that locates in the north-east fringe of Beijing city of China with a mixture of thee types of residential areas and complex background cover types including grassland, woodland, river, pond, main road, bare ground and bare farmland (Figure 1). Representative training sites for the residential class (including three types of residential areas) and background ((including water bodies, grass land, wood land, road, bare farmland, barren ground, etc.) were selected through accurate analysis with the reference to multi-spectral images covering the same area by using a polygon-based approach.



Figure 1. The test image (IKONOS panchromatic band at 1 meter resolution 2719×2449 pixels)

#### 3.1 Optimal parameter value of window size

In this paper, different window sizes (5×5 to 29×29) were tested for deriving every texture feature. The 29×29 was selected as the upper limit of window size because the obvious ‘window problem’ was observed for those with greater window sizes. The JM-distance between residential class and its background classes was calculated on each texture measurement with different window sizes. Figure 2 shows the statistical results, on which it is clear that except *MEAN* (17×17), *SD* (9×9) and *ED*, the optimal window size for all texture bands is 25×25 pixels, supported by the largest JM-distance between residential class and background. For *MEAN* and *SD*, although the JM-distances were peaked with different window size, the actual differences to those with the 25×25 window were quite minimal. This also applied to *ED*, which is peaked with the 29×29 window with only minimal difference from the 25×25 window. Therefore, the 25×25 window size is selected as the optimal window size for deriving texture features for the residential class.

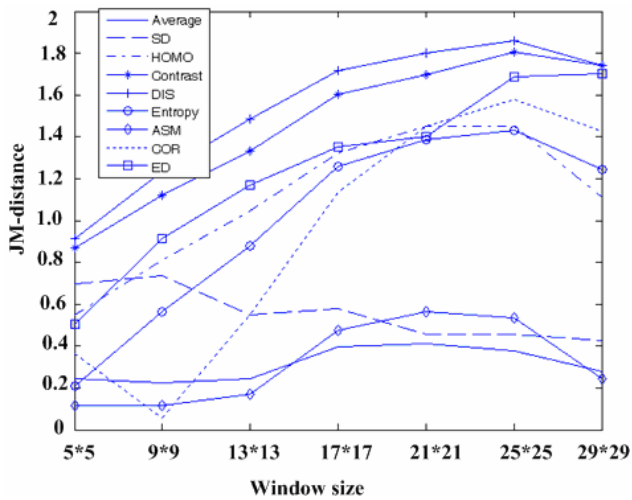


Figure 2. JM-distance between residential and background classes on different textural features with respect to window size

### 3.2 Optimal parameter value of quantization

Four different quantization schemes 16, 32, 64 and 256 grey levels were tested for GLCM texture features. Figure 3 shows JM-distance variation with respect to the pixel grey levels. The result shows that the quantization level dose not have significant impact on *CON*, *DIS* and *SD* bands, and appears to have negative impact on the other texture features including *ENT*, *HOMO*, *ASM* and *COR*. To balance the accuracy and demand on computation resources, we chose a quantization level of 32.

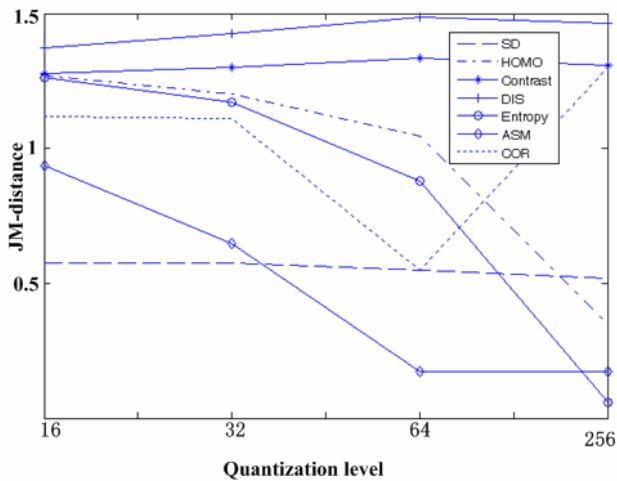


Figure 3. JM-distance between residential and background classes on different textural feature with respect to quantization level

### 3.3 Optimal parameter value of displacements

In this study, displacements of 1,3,5 and 7 pixels were tested as shown in Figure 4. In general there is a tendency that JM-distance decreases with the increasing displacement. Since it appears that low displacement yield generally better results (greater JM-distances) for most texture bands, we therefore selected one as displacement in texture computation.

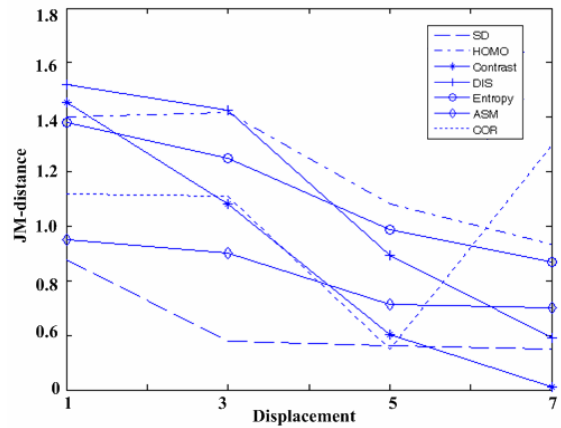


Figure 4. JM-distance values between residential class and background class on different textural feature image with respect to displacement

### 3.4 Optimal parameter value of orientation

To assess the impact of various orientation on the derived texture measures, we examined their separability with the variations on orientation of 0°, 45°, 90°, 135° and the average of four orientations. Figure 5 shows that, except for *SD*, JM-distances on average orientation are significantly greater than on the others.

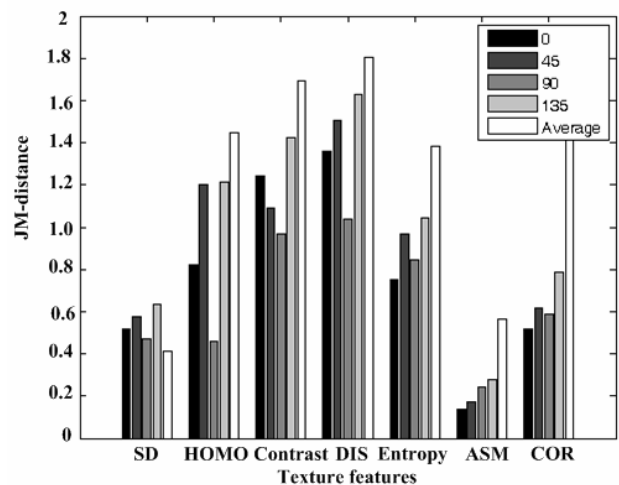


Figure 5. JM-distance values between residential and background classes on different textural features with respect to orientation

Table 1 summarizes the optimal parameters selected for deriving texture measures in this study.

As the parameters of each texture feature have been selected, nine texture images can be obtained from the original IKONOS Panchromatic image. The nine texture features can be separated into five categories according to their properties, namely, the ‘contrast’ group (*CON*, *DIS* and *HOMO*), the ‘orderliness’ group (*ASM* and *ENT*), the ‘edge’ group (*ED*), the ‘mean’ group (*MEAN*) and the ‘descriptive statistics’ group (*SD* and *COR*). To understand the distribution of different kinds of land cover types on each texture space image better, we plot the clusters based on the training samples. Figure 6 to figure 9 shows the cluster result.

Figure 6 shows *ED* and *MEAN* statistics of nine land cover types. Generally speaking, bare ground shows the highest *MEAN* value, while water bodies show the lowest. In between there are numerous 'confusing' classes including three types of residential area, farmland, grassland and woodland. It is obvious that the *MEAN* alone does not provide enough variance to distinguish residential areas from their background. Old urban and rural residential areas show greater *ED* values as their buildings are assembled densely. Roads and cars on the road have clear edges resulting in a high *ED* value. New urban residential areas have sparse buildings, thus their *ED* values are smaller than the other two types of residential areas. Trees in woodland often show clear crown and shadows on high-resolution images, thus is more likely to detect edge point with this cover type. Other background classes such as water, grassland, bare farmland and bare ground have an *ED* value close to zero. Thus, it is clear that *ED* is a good candidate for the detection of residential areas with the background except road and wood land.

Figure 7 presents the contrast group to distinguish residential areas and background. New urban residential area, road, rural residential area, old urban residential area and wood land show more contrast than water, grassland, bare farmland and bare ground.

Figure 8 shows orderliness group in describing pixel variation. All three kinds of residential areas have less order or uniform surface: woodland and road show medium uniform surface, while water, grassland, bare farmland and bare ground represent a uniform surface.

Figure 9 uses *SD* and *COR* to describe differences of residential areas and their background. It can be seen that new built urban residential area, old urban residential area, rural residential area, road and woodland all show greater *SD* values, which means that the pixel *DN* values are more diversified. In contrast, bare ground, grassland, water and barren farmland all show smaller *SD* values. All three types of residential areas are characterized with smaller *COR* values than the background classes, suggesting more discrete and less dependent spectral distribution.

#### 4. CONCLUSIONS

In this paper, we investigated methods for selecting and evaluating texture parameters (window size, quantization level, displacement and orientation) for the identification of residential areas based on JM-distance. grey level co-occurrence matrix (GLCM) and edge density (ED) approaches with candidate nine texture measurements (contrast, homogeneity, dissimilarity entropy, energy, mean, standard deviation, correlation and edge density) is selected as candidate texture measurements. The texture parameters are selected based on Jeffries-Matusita distance (JM distance) between residential and its background in corresponding texture space. IKONOS panchromatic imagery has been used as example and the optimal texture parameters were selected by using the proposed method. Further studies will be focused on the selection of optimal texture combination to improve the residential classification results.

#### ACKNOWLEDGEMENT

This project is financed by two items of the National Natural Science Foundation of China (Contract No. 40337055 and Contract No. 40501062).

#### REFERENCES

- Anys, H. and He D.C., 1995. Evaluation of textural and multipolarization radar features for crop classification, *IEEE Transactions of Geoscience and Remote Sensing*, 33(5): 1170-1181.
- Coburn, C.A., Roberts, A.C.B., 2004. A multiscale texture analysis procedure for improved forest stand classification, *International Journal of Remote Sensing*, 20 October, 25(20), 4287-4308.
- Connors, R.W and Harlow, C.A.,1978. Equal probability quantizing and texture analysis of radiographic images, *Computer Graphics Image Processing*, 8, 447-463.
- Canny J.F. 1986. A computational approach to edge detection. *IEEE Transactions on Pattern Analysis and Machine Intelligence*, 8(6): 679-698.
- Gong, P., 1991. A comparison of spatial feature extraction algorithms for land-use classification with SPOT HRV Data, *Remote Sensing of Environment*, 40, 137-151.
- Haralick, R.M. 1979. Statistical and structural approaches to texture, *Proceedings of the IEEE*, 67, 786-804.
- Karathanassi, V., Iossifidis, CH., and Rokos, D., 2000. A texture-based classification method for classifying built areas according to their density, *International Journal of Remote Sensing*, 21(9), 1807-1823.
- Myint, S.W. and Lam, N., 2005. A study of lacunarity-based texture analysis approaches to improve urban image classification, *Computer, Environment and Urban Systems*, 29, 501-523.
- Shaban, M.,A., and Dikshit, O., 2001. Improvement of classification in urban areas by the use of textural features: the case study of Lucknow city, Uttar Pradesh, *International Journal of Remote Sensing*, 22(4), 565-593.
- Soh, L.K. and Tsatsoulis, C., 1999. Texture analysis of SAR sea ice imagery using grey level co-occurrence matrices, *IEEE Transactions on Geoscience and Remote Sensing*, 37(2), 780-795.
- Swain, P.H. and Davis S.M.,1978. Remote Sensing: The quantitative approach, *New York: McGraw-Hill*,
- Zhang, Q., Wang, J., Gong, P., and Shi., P, 2003. Study of urban spatial patterns from SPOT panchromatic imagery using textural analysis, *International Journal of Remote Sensing*, 24(21), 4137-4160.

	MEAN	SD	HOMO	CON	DIS	ENT	ASM	COR	ED
Window size	17×17	9×9	25×25	25×25	25×25	25×25	25×25	25×25	25×25
Grey levels	-	Constant	16	64	64	16	16	256	-
Displacement	-	1	3	1	1	1	1	7	-
Orientation	-	135°	Average	Average	Average	Average	Average	Average	-

Table 1. Optimal parameters for each texture features

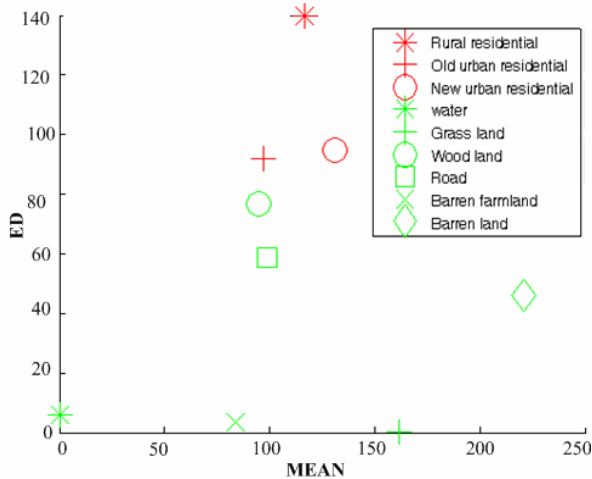


Figure 6. Cluster of land cover types in the space defined by MEAN and ED

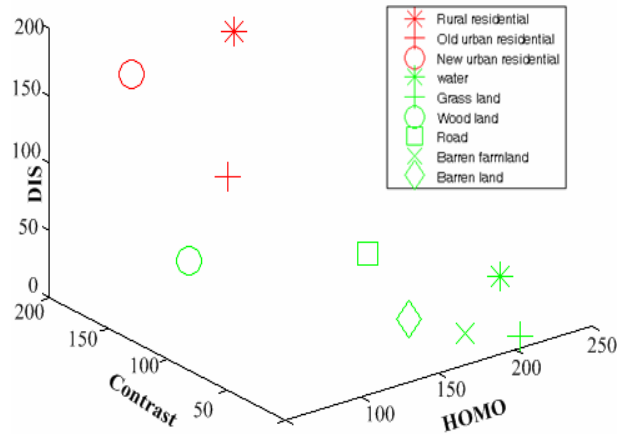


Figure 7. Cluster of land cover types in the contrast space

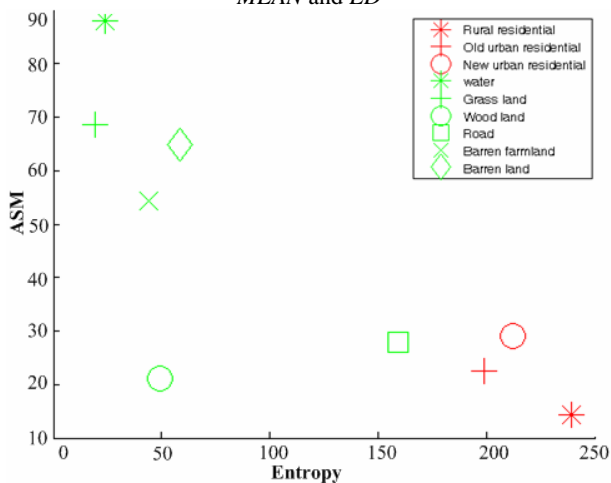


Figure 8. Cluster of land cover types in the orderliness space

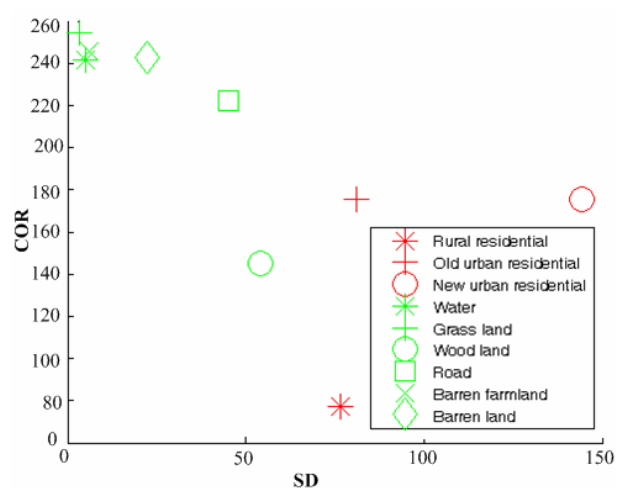


Figure 9. Cluster of land cover types in the space defined by SD and COR